

Estimation of Sea Surface Temperature Using Infrared Image Data of Geostationary Meteorological Satellite (GMS)

Akihiro Uchiyama*, **Hiroshi Fujimura**** and **Toshiro Yogai*****

Abstract

A new method to correct infrared image data of GMS is described and the test results obtained by the new method are shown in this report.

In the current operational system of Japan Meteorological Satellite Center (JMSC), an atmospheric correction for infrared image data of GMS is performed on the basis of an empirical formula and climate precipitable water amount. In a new method, the results of objective analysis for numerical prediction is used as a vertical profile of temperature and water vapor, and a value of atmospheric correction is calculated by the method of solving a radiative transfer equation. We applied this method to four cases and estimated sea surface temperature (SST).

The results shows that new method tends to cause systematic error over a wide range of areas and it is found that the error of clear or cloud free radiance observed by a satellite and that of atmospheric correction are amplified and cause a large error in the estimated SST. This feature is inherent and suggests that it is very difficult to estimate SST from only one infrared channel.

In order to estimate SST with the accuracy less than 0.5 K, both the clear radiance and the amount of atmospheric correction should be determined with the accuracy less than 0.1 K. Furthermore, in order to remove the atmospheric effect by the own measurement, it is to be desired that radiances should be measured in a number of wave number region.

1. Introduction

For the purpose of better understanding on climate and long-term prediction, a variety of projects are being carried out and planned. The required accuracy to measure sea surface temperature (SST) is 0.2 to 0.5 K for monthly mean value. Since a meteorological satellite was launched, homogeneous data can be obtained over a wide range of

area and in a short period of time. The satellite data has been utilized to estimate SST because of these advantages. Especially, since the space resolution of infrared image data is superior to the other instrument, infrared image data is often utilized for retrieving SST.

Japan Meteorological Satellite Center has operationally derived mean SST for ten days, since April in 1978. The order of error is about 1.5 to 2.5 K. In the current operational system, the amount of atmospheric correction is calculated on the basis of an empirical formula and climatic precipitable water vapor amount (Inoue, 1979).

* Japan Meteorological Satellite Center System Engineering Division.

** Japan Meteorological Satellite Center Satellite Operations Division (Present affiliation: Science and Technology Agency).

*** Japan Meteorological Satellite Center Neph-analysis Division.

We have developed a new method to remove the atmospheric effect from the observed infrared image data and the current operational method will be replaced by the new one. The three major points are changed. Firstly, the climatic vertical profile of atmospheric temperature and water vapor is replaced by the result of objective analysis for numerical prediction, which are given every 2.5° latitude \times 2.5° longitude. Secondly, the amount of atmospheric correction is calculated by the method of solving a radiative transfer equation. Thirdly, cloud free radiances are extracted from the histogram data in the box of 0.25° latitude \times 0.25° longitude.

In this report, we described the new method to correct atmospheric effect and the test results obtained by the new method. The test results show that the new method does not necessarily improve SST derived from GMS infrared image data. In the section 4, the causes of errors are discussed in detail.

2. Method of SST estimation

When we retrieve SST from infrared radiance observed by the satellite, the effect of atmosphere must be removed from a clear or cloud free radiance, which is not affected by the radiance from cloud. This process is called 'atmospheric correction'.

(a) vertical profile

In order to correct the atmospheric effect, we need a vertical profile of atmosphere. It is impossible to infer an accurate vertical structure of atmosphere from the only one infrared window channel. We depend on the other source of data to give the vertical structure of atmosphere. In the current

operational system, monthly climate values, which are prepared every 5° latitude \times 5° longitude over a range of observation area covered by GMS, has been used. In the new method, the result of objective analysis for numerical prediction is used as a vertical profile of temperature and water vapor. This data contains atmospheric temperature between surface and 10 mb level and relative humidity between surface and 400 mb level, every 2.5° latitude \times 2.5° longitude.

(b) atmospheric correction

The current operational method to calculate the amount of atmospheric correction is based on the empirical formula which is dependent on a cosine of satellite zenith angle, a column precipitable water amount, and an observed brightness temperature (T_{BB}). At the beginning of the operation of the current system, coefficients of the empirical formula were determined from the data set calculated theoretically (Inoue, 1979). Since November in 1982, the dependence on observed T_{BB} has been neglected to linearize the equation and its coefficients have been determined by the least squares method from the truth data of SST observation and the column precipitable water amount observed by the radiosonde.

In the new method, the amount of atmospheric correction is not calculated directly because the atmospheric correction is dependent on not only the atmospheric vertical structure but also the sea surface temperature. The schematic view of a principle to estimate SST is shown in Fig. 1. Given a vertical profile of atmosphere and a number of SST (T_{Si} , $i=1, \dots, N$), the observed radiances or brightness temperature (T_{BB}^o , $i=1, \dots, N$) are precalculated and a look-up

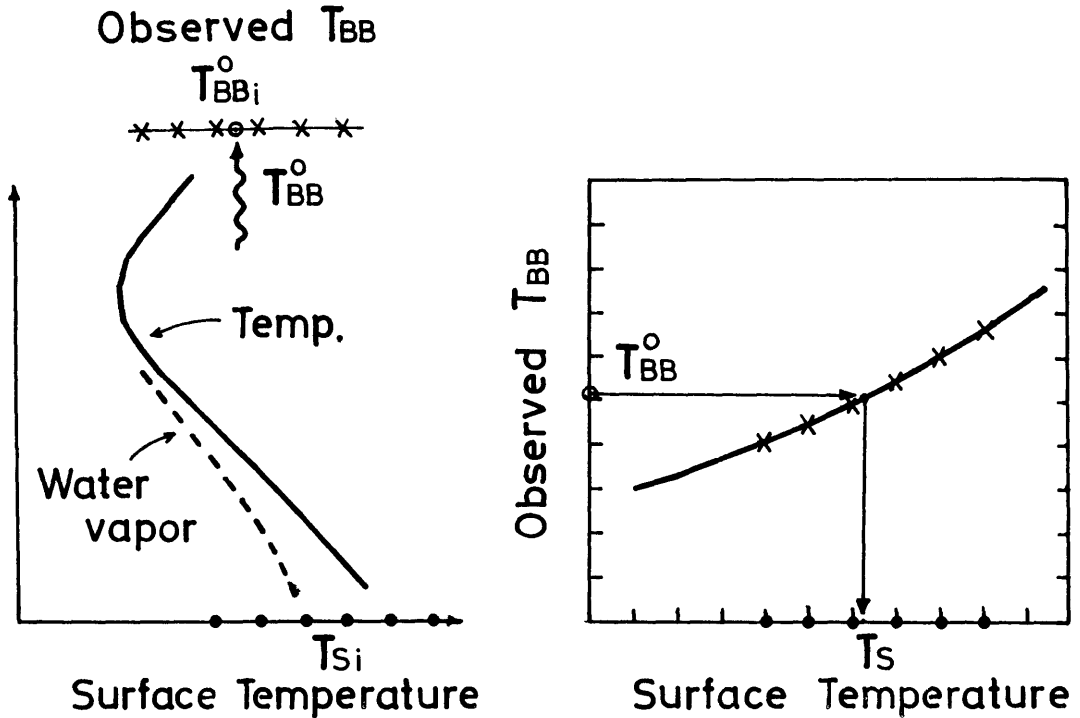


Fig. 1 The schematic view of a principle to estimate SST. Given a vertical profile and a number of SST (T_{Si} , $i=1, \dots, N$), the observed $T_{BB}^o_i$ ($i=1, \dots, N$) are calculated. Using a look-up table inversely, SST is estimated from the clear T_{BB} observed by the satellite. Note that the amount of atmospheric correction is dependent on not only the atmospheric profile but also the surface temperature.

table of the observed $T_{BB}^o_i$ ($i=1, \dots, N$) for the given T_{Si} ($i=1, \dots, N$) is made. This T_{BB} to be observed monotonously increases with the increase of SST. Using this look-up table inversely, SST is estimated from the clear T_{BB} observed by the satellite.

(c) radiative transfer scheme

The radiative transfer scheme to calculate infrared radiance in the range of $11 \mu\text{m}$ atmospheric window is developed on the basis of the method developed by Weinreb and Hill (1980).

On the assumption of a plane-parallel atmosphere, local thermodynamic equilibrium and neglect of scattering process, the up-

welling radiance $I(\nu)$ at wave number ν can be calculated numerically by following equation,

$$I(\nu) = B(T_s, \nu) \cdot \tau(Z_s, \nu) + \int_{Z_s}^{Z_{st}} B(T(Z), \nu) \frac{d\tau(Z, \nu)}{dZ} dZ \quad (1)$$

where $B(T, \nu)$ is Planck's function at temperature T and wave number ν , $\tau(Z, \nu)$ is transmittance between the satellite and the altitude Z , and the subscript 's' and 'st' indicate that a quantity is to be evaluated at the earth's surface and a satellite, respectively. In order to apply the above equation to a spectral interval of a broad-band instrument, it must be convoluted with the spectral

response function $\phi(\nu)$ of the interval. The radiance $\tilde{I}(\nu)$ that would be measured in any of these intervals is then given by

$$\tilde{I}(\nu) = \frac{\int_{\Delta\nu} \phi(\nu) \cdot I(\nu) d\nu}{\int_{\Delta\nu} \phi(\nu) d\nu} \quad (2)$$

Weinreb and Hill divided the full spectral interval into subintervals (30 cm^{-1}) with the rectangular response function. Then, the radiance $\tilde{I}(\nu)$ is approximated by weighted mean of each subinterval radiance $I(\nu_i)$,

$$\tilde{I}(\nu) = \frac{\sum_i \phi_{\nu_i} \cdot I(\nu_i) \cdot \Delta\nu_i}{\sum_i \phi_{\nu_i} \cdot \Delta\nu_i} \quad (3)$$

where ϕ_{ν_i} is height of rectangular response function, and $\phi_{\nu_i} \cdot \Delta\nu_i$ is equal to the area of original response function in each subinterval.

In each subinterval, the transmittance of the atmosphere is treated as a product of the transmittances of the atmospheric absorbing constituents. In the $11 \mu\text{m}$ region, the absorbing constituents are water vapor and the "uniformly mixed gases" (McClatchy et al., 1972), principally carbon dioxide. Water vapor spectral lines and continuum dominate the absorption in this spectral region. For calculating transmittances of spectral lines, Weinreb and Hill used the method of Weinreb and Neuendorffer (1973). This method treats the atmosphere as a succession of homogeneous layers, in each of which the pressure, temperature and mixing ratio are constant. This method need the transmittance for homogeneous path. Weinreb and Hill choose a polynomial representation similar to that suggested by Smith (1969). The following polynomial expression is used,

$$\ln(-\ln(\tau_j)) = \sum_{i=1}^{14} C_i(\nu_j) X_i \quad (4)$$

where τ_j is transmittance averaged over the rectangular subinterval,

$$X_1 = 1, \quad X_2 = 0.1 \cdot \ln(U \cdot T / 273),$$

$$X_3 = \ln(P/1000), \quad X_4 = \ln(T/273),$$

$$X_5 = X_2 \cdot X_3, \quad X_6 = X_2 \cdot X_4, \quad X_7 = X_2^2,$$

$$X_8 = X_4 \cdot X_7, \quad X_9 = X_3 \cdot X_4, \quad X_{10} = X_2 \cdot X_7,$$

$$X_{11} = X_4 \cdot X_6, \quad X_{12} = X_4^2, \quad X_{13} = X_3 \cdot X_6,$$

$$\text{and } X_{14} = X_3 \cdot X_7,$$

U : water vapor amount

P : total pressure

T : temperature

These coefficients $C_i(\nu_j)$ are calculated in every 30 cm^{-1} interval between 760 cm^{-1} and 1000 cm^{-1} . The procedure for calculating the scaled amount of U in each layer is necessary. We use Newton method and solve eq. (4) with respect to X_2 .

For the water vapor continuum, the following formula of Roberts et al. (1976) is used;

$$k_\nu(T) = C_\nu(T)(P_{\text{H}_2\text{O}} + \gamma \cdot (P - P_{\text{H}_2\text{O}})) \quad (5)$$

$$C_\nu(T) = C_\nu^0(T=296) \exp\left(T_0 \left(\frac{1}{T} - \frac{1}{296}\right)\right)$$

$$C_\nu^0 = a + b \exp(-\beta \cdot \nu)$$

$$T_0 = 1800 \text{ K}$$

$$a = 1.25 \times 10^{-22} \text{ mole}^{-1} \text{ cm}^2 \text{ atm}^{-1}$$

$$b = 2.34 \times 10^{-18} \text{ mole}^{-1} \text{ cm}^2 \text{ atm}^{-1}$$

$$\beta = 8.30 \times 10^{-3} \text{ cm}$$

$P_{\text{H}_2\text{O}}$: water vapor pressure

where ν is wave number. Weinreb and Hill neglected the second term of eq. (5), but we do not neglect this term.

The uniformly-mixed gases comprise CO_2 ,

N_2O , CO , CH_4 , and O_2 . CO_2 absorbs weakly in the $11\ \mu m$ window. The method of calculating transmittances is taken from LOWTRAN (Selby et al., 1978, Kneizys et al., 1980).

According to Weinreb and Hill, the error of their method probably less than $1\ mW / (cm^2 \cdot sr \cdot cm^{-1})$.

(d) clear radiance

The other point to be changed is a procedure to extract a clear radiance. In the current operational procedure, clear radiance is extracted from the histogram data in the area of 1° latitude \times 1° longitude by the method of the histogram analysis. In the new procedure, it is extracted from the histogram data in the area of 0.25° latitude \times 0.25° longitude.

3. Test results of SST estimation

The sea surface temperatures of the first ten days in January, April, July and October in 1985 are estimated in the area between $110^\circ E$ and $180^\circ E$ on the northern hemisphere.

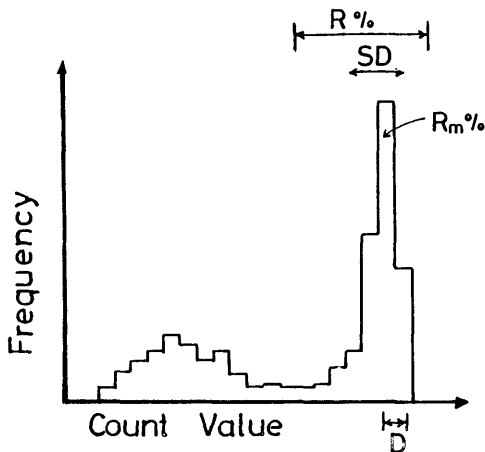


Fig. 2 Parameters for checking the peak of the histogram in the part of the higher temperature. We select a sharp and high peak in the part of the higher temperature as a cloud free data.

The infrared image data observed by $GMS-3$ at 00Z, 06Z, 12Z and 18Z are used. The clear T_{BB} is extracted from the histogram data in the area of $0.25^\circ \times 0.25^\circ$. The first peak of the histogram in the part of the higher temperature is checked by using the following parameters (see Fig. 2),

R : the ratio of the number of element in that peak to the number of total elements,

Rm : the ratio of the number of element in the mode level in that peak to the number of elements in that peak,

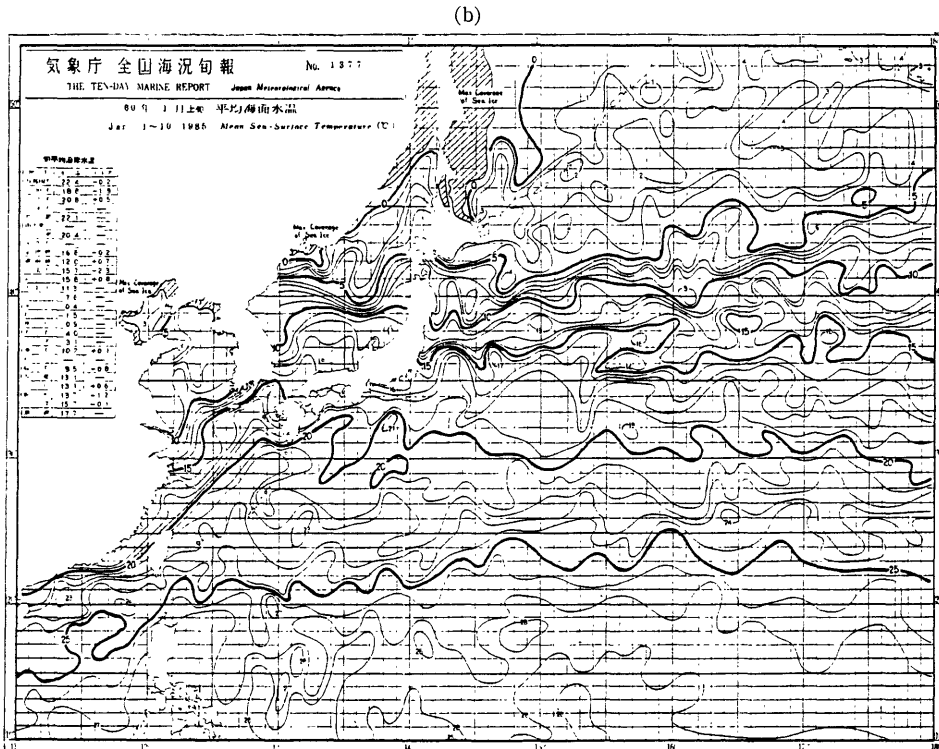
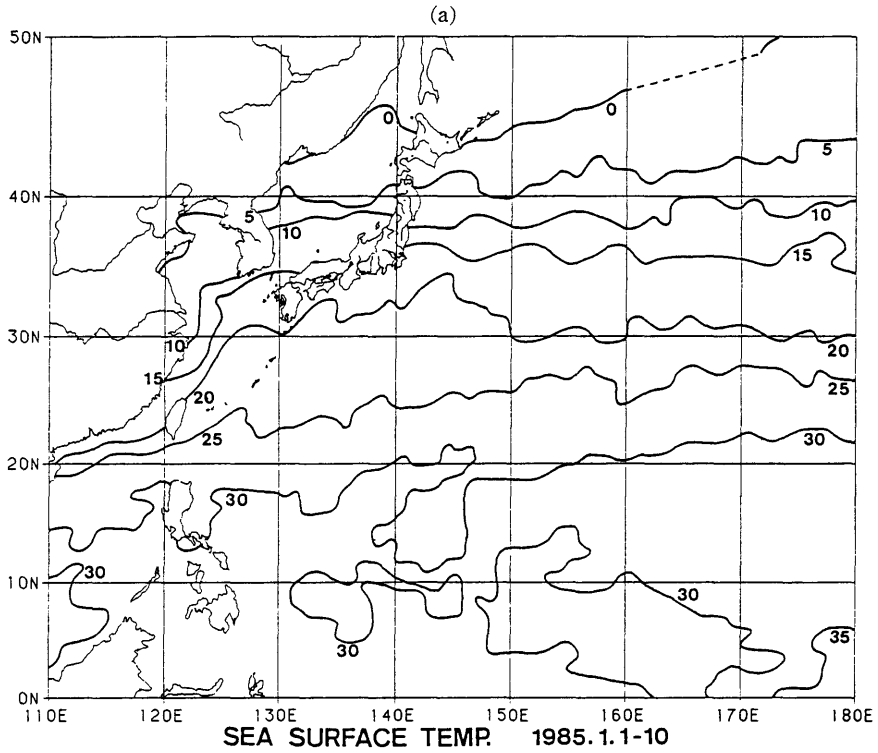
SD : standard deviation of elements in that peak,

D : difference between maximum count value and mode one in that peak,

T_{th} : threshold value for a estimated sea surface temperature.

We adopt $T'-2$, as the threshold value, where T' is a calculated T_{BB} on the assumption that the surface temperature is equal to the atmospheric temperature at the lowest level. If R is greater than or equal to 50 percents, Rm is greater than or equal to 40 percents, SD is less than or equal to 2, D is less than 3, and SST estimated from mean T_{BB} of the first peak of the higher temperature part is greater than T_{th} , then we regard the first peak of the higher temperature part as the cloud free peak of the histogram. In short, we select the sharp and high histogram peak in the higher temperature part as the cloud free data. This method is not a operational one but the basic idea of the operational one is similar to this one.

Since the vertical profile is given on the grid point every $2.5^\circ \times 2.5^\circ$, the amount of



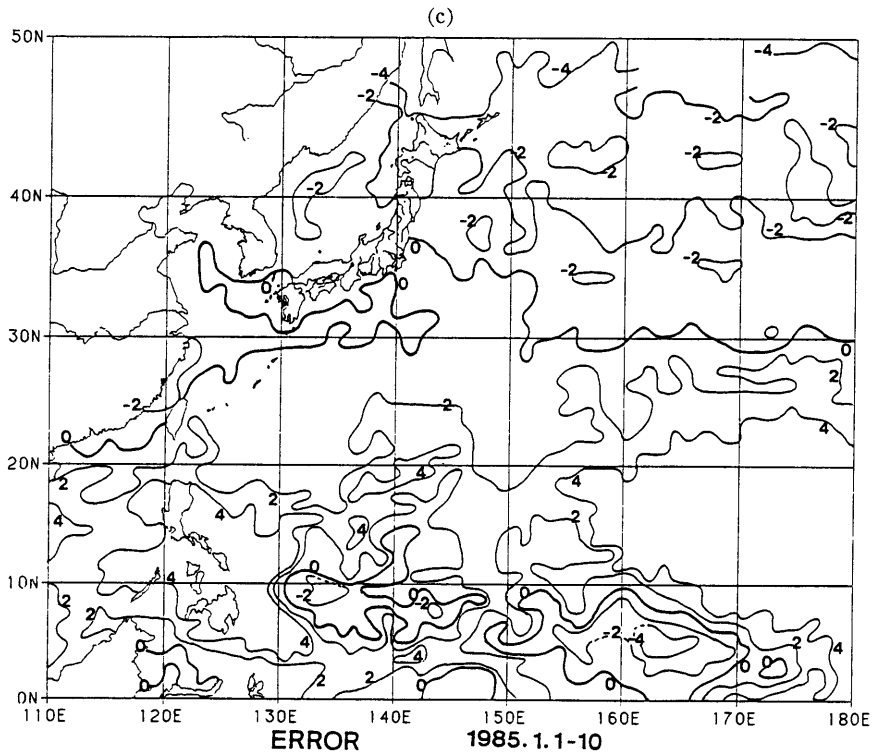


Fig. 3 (a) The sea surface temperature of the first ten days of January in 1985 estimated from GMS-3 data. (b) The Ten-Day Marine Report produced by Japan Meteorological Agency on the basis of ship measurements mainly. (c) Difference between (a) and (b) ((a)-(b)). The regions where differences are greater than 2K appear over the wide range of areas.

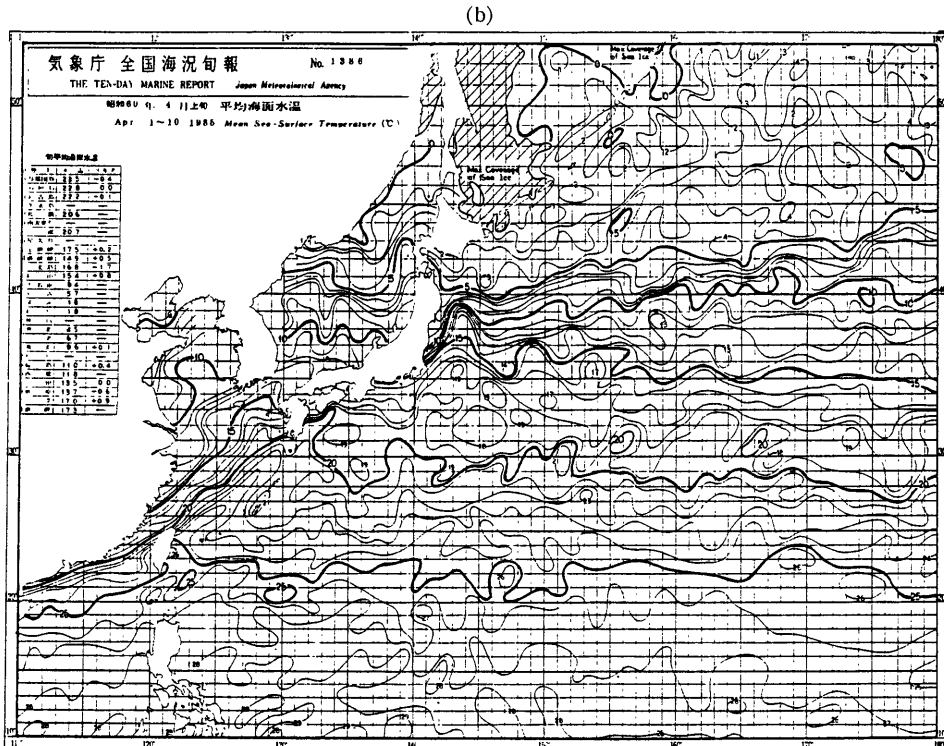
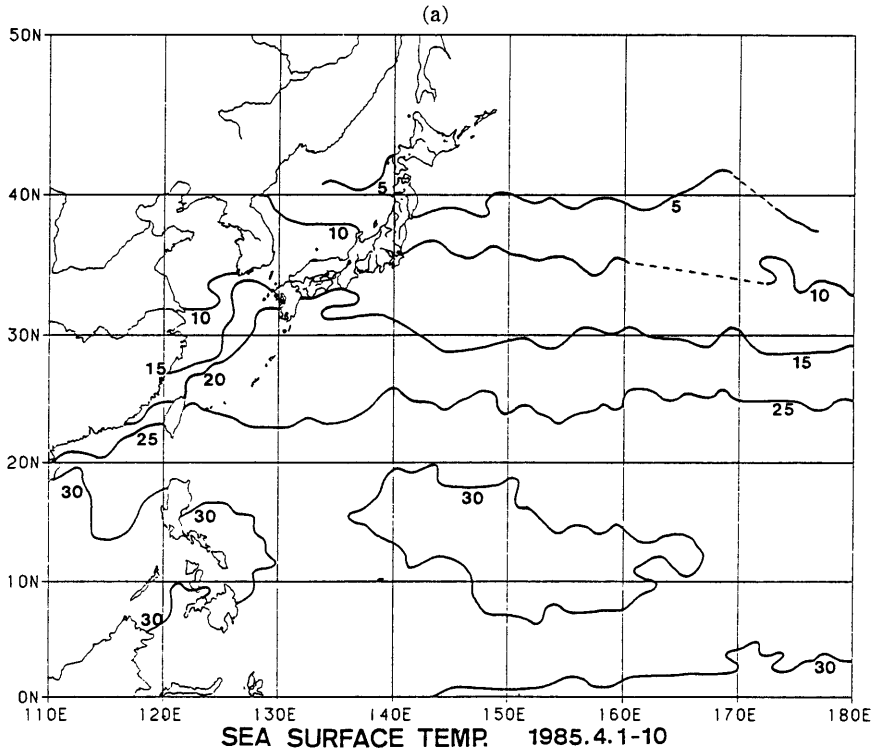
atmospheric correction in the box is interpolated from the data of the four corners of box. The transmittances of water vapor continuum are calculated using $\gamma=0.005$.

Fig. 3 (a), (b), and (c) show the sea surface temperature of the first ten days of January in 1985 estimated from GMS-3 data, the Ten-Day Marine Report produced by Japan Meteorological Agency, which is based on mainly ship data, and the differences between the former SST and the latter SST, respectively. There are some features in Fig. 3 (c). The regions where differences are greater than 2.0 K appear over a wide range of area. There is a tendency that differences are negative or the estimated

SSTs are less than the Ten-Day Marine Report in the region of the higher latitude zone. Comparing Fig. 3 (c) with photographs during the same period, the negative errors in the lower latitude appear in the cloudy areas, and the positive errors in the lower and middle latitude appear in the clear areas.

Fig. 4 is the same one as Fig. 3 except for April. In this case, the tendencies of error are similar to that in January. SST could not be estimated in the latitude zone higher than 40°N.

Fig. 5 is the same one as Fig. 3 except for June. SST cloud not be estimated in the latitude zone higher than 40°N. In this case, the negative errors appear almost all



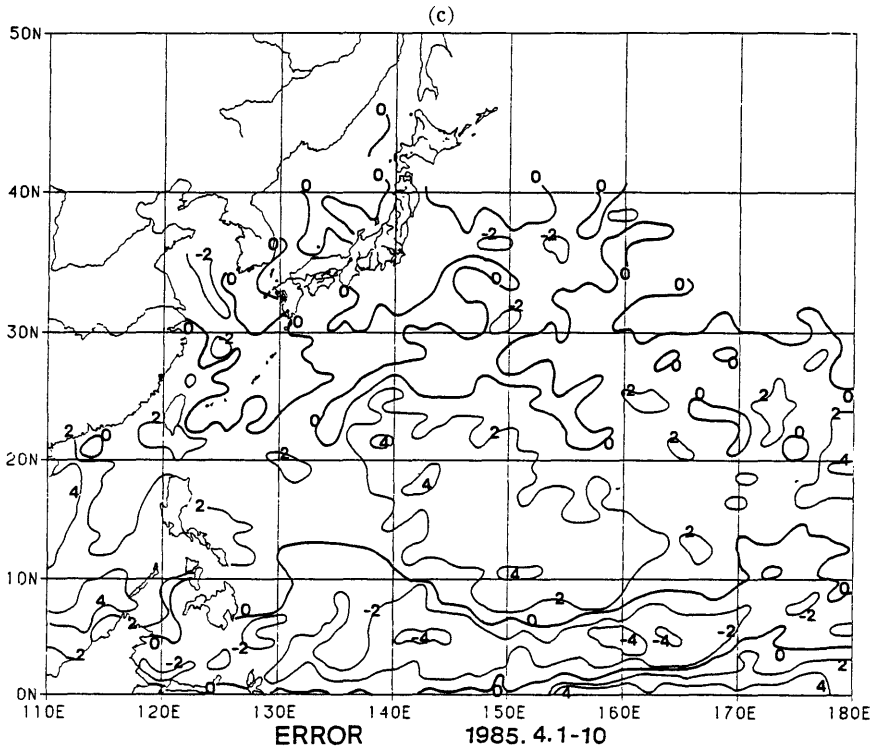
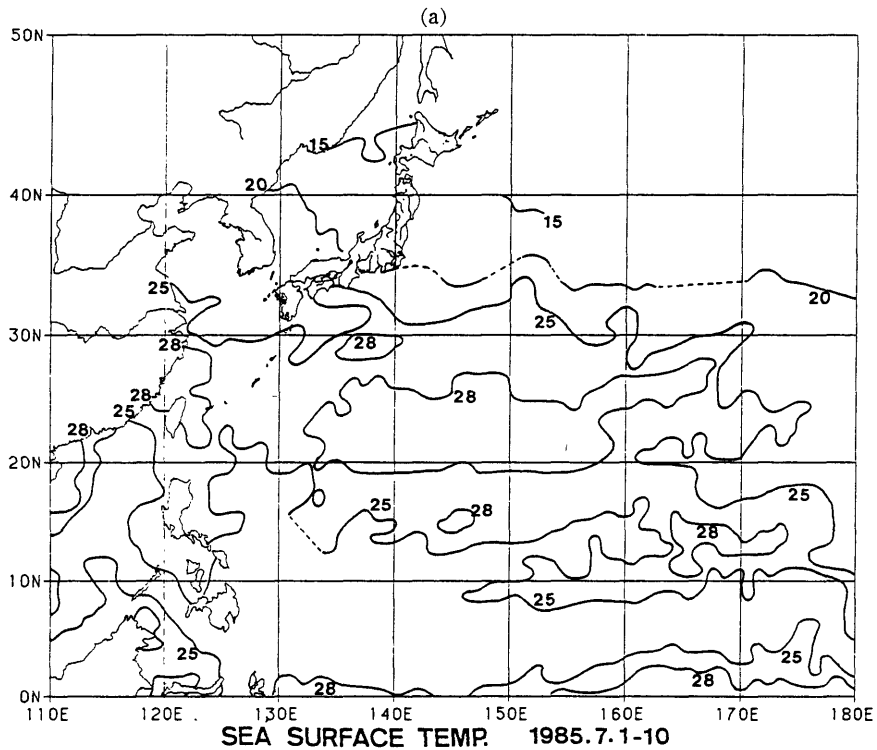
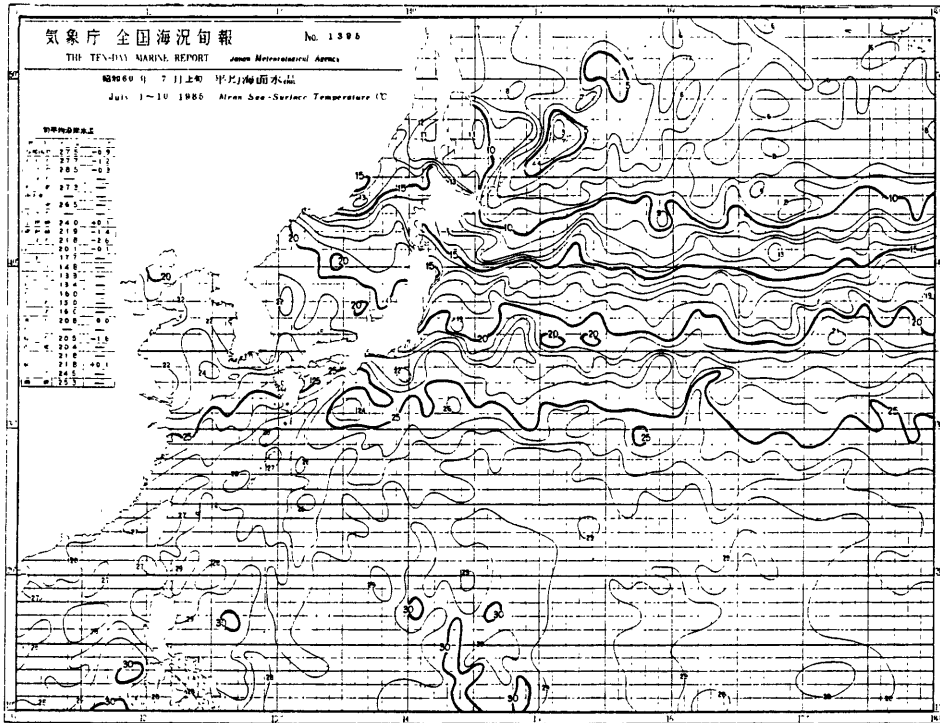


Fig. 4 As in fig. 3, except for April. Tendencies of difference are similar to those in January.



(b)



(c)

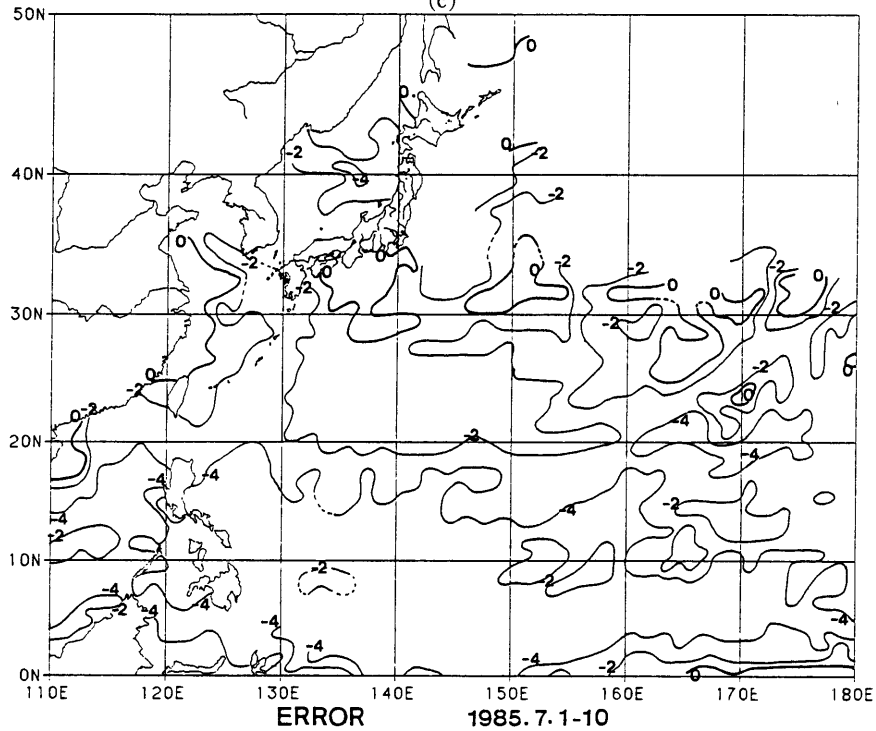
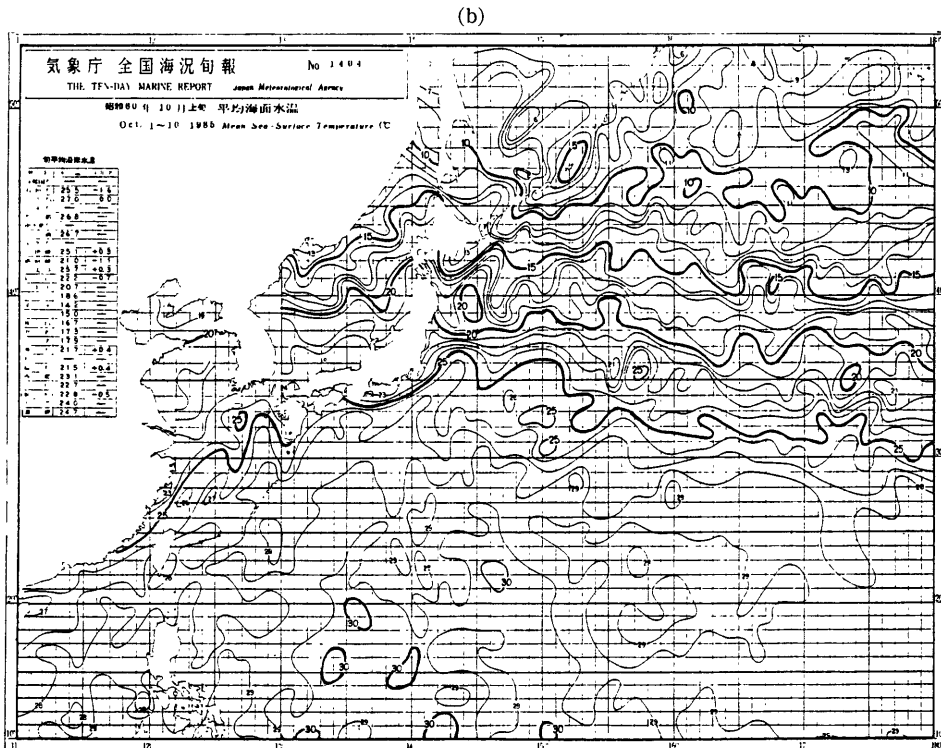
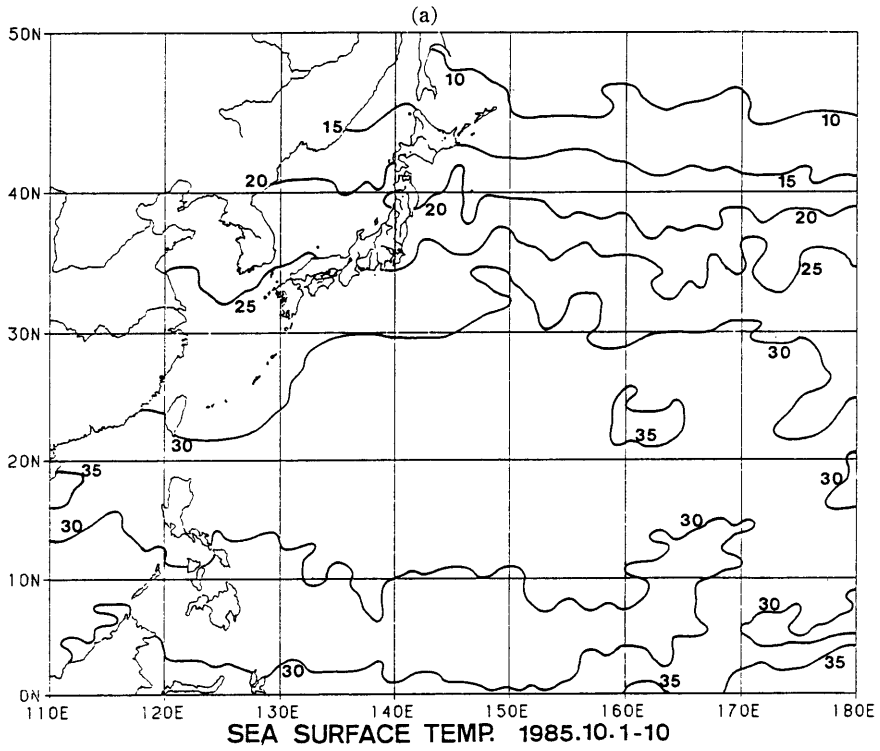


Fig. 5 As in fig. 3, except for July. The negative differences, which means that SST estimated from GMS-3 data is lower than that of the Ten-Day Marine Report, appear almost all over areas.



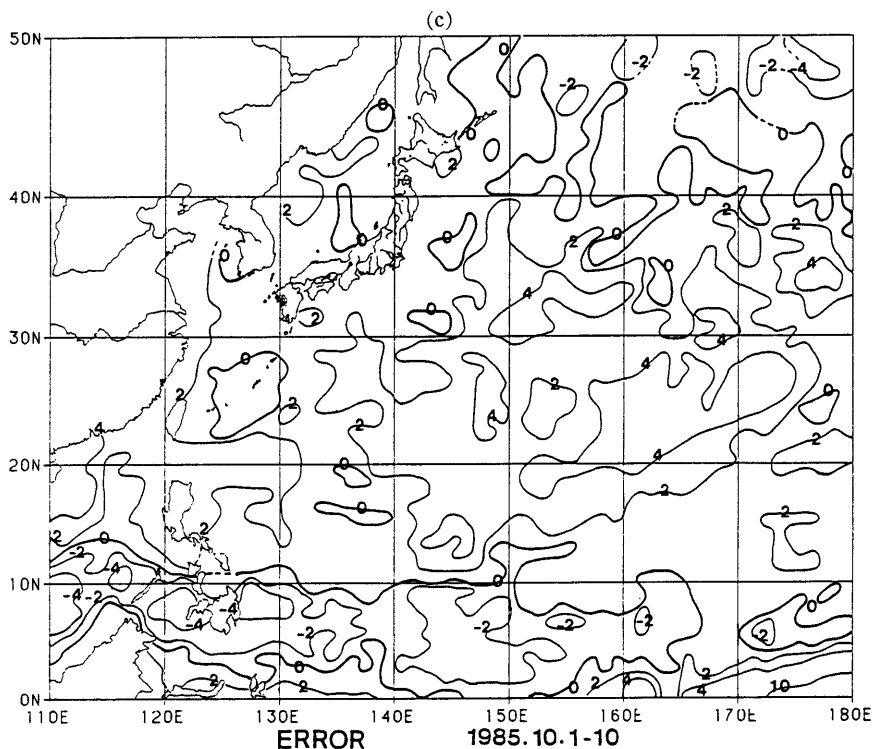


Fig. 6 As in fig. 3, except for October. Tendencies of difference are similar to those in January and April.

over areas. This tendency is small in the clear areas in the middle latitude.

Fig. 6 is the same one as Fig. 3 except for October. The tendencies of error in October are similar to that in January and April.

In every case, the large differences between SST estimated from GMS data and Ten-Day Marine Report appear over a wide range of area. They sometimes exceed 5 K. These SSTs cannot be utilized for the quantitative analysis of SST.

4. Discussion

The error of SST estimated from GMS infrared image data is caused by the following factors.

(1) clear radiance and clear T_{BB}

(2) radiative transfer scheme

(3) calibration of the radiometer on GMS

(4) vertical profile of temperature and water vapor

In this section, we discuss these factors in detail.

(a) clear radiance and clear T_{BB}

It is difficult to estimate the magnitude of error in the clear radiance and T_{BB} precisely. We cannot avoid the error to a degree of 1 to 2 count values.

If the size of cloud is less than a field of view, we cannot remove the effect of cloud contamination. The field of view for infrared channel on GMS is 6 km×6 km at a sub-satellite point. The histograms of elements in 1° latitude×1° longitude for both infrared and visible channel are shown in

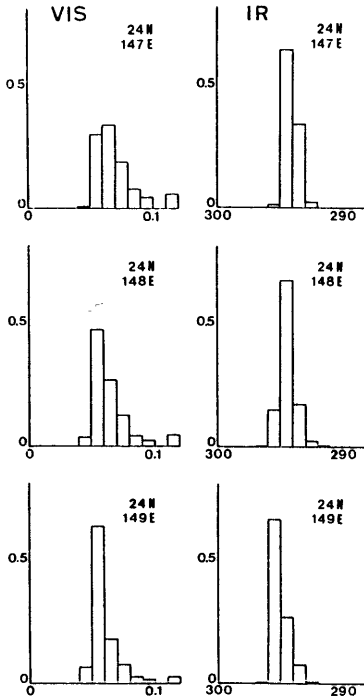


Fig. 7 The histogram of elements in 1° latitude \times 1° longitude for both visible and infrared channel. The center of positions are $(24^\circ\text{N}, 147^\circ\text{E})$, $(24^\circ\text{N}, 148^\circ\text{E})$, and $(24^\circ\text{N}, 149^\circ\text{E})$. If we would check infrared histogram only, the three histogram are probably regarded as clear. Judging from visible data, the above two histogram are contaminated by cloud, and mode values of the above two infrared histogram are 1 K lower than that of the third one.

Fig. 7; center of areas are $(24^\circ\text{N}, 147^\circ\text{E})$, $(24^\circ\text{N}, 148^\circ\text{E})$, and $(24^\circ\text{N}, 149^\circ\text{E})$. If we would check infrared histogram only, these three histograms are probably regarded as clear. However, judging from visible histograms, the above two histograms for visible channel are obviously contaminated by cloud. The mode values for the above two histograms for infrared channel are 1.0 K as low as that of the third one. The existence of cloud in the field of view partially ex-

plains that the SSTs estimated from GMS-3 data is lower than the truth data in the higher latitude zone and in the cloudy area of lower latitude.

(b) radiative transfer scheme

According to Weinreb and Hill (1980), the error of radiative transfer scheme is less than $1 \text{ mW}/(\text{cm}^2 \text{ sr cm}^{-1})$; $1 \text{ mW}/(\text{cm}^2 \text{ sr cm}^{-1})$ correspond to 0.6 K in the vicinity of 300 K.

For the purpose of investigating the error of radiative transfer model, we compared the calculated T_{BB} with the observed clear T_{BB} from October in 1984 to October in 1985. The radiances were calculated using SSTs of the Ten-Day Marine Report and the radiosonde data at the stations near the coast and on the island. The radiosonde stations are listed on Table 1. The radiosonde data is extrapolated to surface level from the altitude of the station. We extracted the clear T_{BB} near the radiosonde station. The positions which are used for extracting the clear T_{BB} and calculating the radiance are also listed on Table 1.

The transmittance for water vapor continuum is calculated using $\gamma=0.005$ and $\gamma=0.0$.

The clear T_{BB} is extracted using the same method as the estimation of SST except for the threshold value. Instead of the threshold value, the difference between the calculated T_{BB} and the extracted clear one is used; i.e. if difference is less than 10.0 K, the extracted T_{BB} is adopted as the clear one.

The data are divided into four group according to the latitude of the position and the statistics of the difference between the observed T_{BB} and the calculated T_{BB} are calculated every month.

Fig. 8 shows the mean of their differences

Table 1 Radiosonde station and position to use for extracting the clear T_{BB} and calculating the radiance or T_{BB} .

No.	Station Name	No.	altitude (m)	lat. (N) (deg.)	long. (E) (deg.)	specified lat. (N) (deg.)	position long. (E) (deg.)
1	URUP	32186	70	46.1	150.5	46	151
2	TERNEJ	31909	11	45.0	136.7	45	138
3	WAKKANAI	47401	11	45.4	141.7	45	141
4	NEMURO	47420	26	43.3	145.6	43	146
5	VLADIVOSTOK	13960	138	43.1	131.9	42	132
6	MISAWA	47580	39	40.7	141.4	41	143
7	AKITA	47582	10	39.7	140.1	40	139
8	SENDAI	47590	43	38.3	140.9	38	143
9	WAJIMA	47600	6	37.4	136.9	37	136
10	QINGDAO	54857	77	36.1	120.3	36	122
11	YONAGO	47744	8	35.4	133.4	36	133
12	FUKUOKA	47807	14	33.6	130.4	34	129
13	SHIONOMISAKI	47778	75	33.5	135.8	33	136
14	HACHIJOJIMA	47678	153	33.1	139.8	33	140
15	SHANGHAI	58367	7	31.2	121.4	31	123
16	CHICHIJIMA	47971	4	27.1	142.2	27	142
17	TAOYUAN	46697	48	25.0	121.1	26	121
18	NAHA	47936	29	26.2	127.7	26	127
19	MINAMIDAITOJIMA	47945	15	25.8	131.2	26	131
20	ISHIGAKIJIMA	47918	7	24.3	124.2	24	124
21	MINAMITORISHIMA	47991	9	24.3	154.0	24	154
22	HAIKOU	59758	15	20.0	110.4	20	112
23	WAKE	91245	4	19.3	166.7	19	167
24	LAOAG	98223	5	18.2	120.5	18	120
25	XISHADAO	59981	5	16.8	112.3	17	112
26	CLARK AFB	98327	196	15.2	120.6	15	119
27	LEGASPI	98444	19	13.1	123.7	14	124
28	GUAM	91217	111	13.3	144.5	14	145
29	YAP	91413	17	9.5	138.1	9	137
30	KWAJALEIN	91366	8	8.7	167.7	8	167
31	KOROR PALAU	91408	33	7.3	134.5	7	133
32	TRUK	91334	2	7.5	151.9	7	152
33	MAJURO	91376	3	7.1	171.4	7	172
34	KOTA KINABALU	96471	3	6.0	116.1	6	114
35	PONAPE	91348	46	7.0	158.2	6	158
36	BRUNEI	69315	15	4.9	114.9	5	114

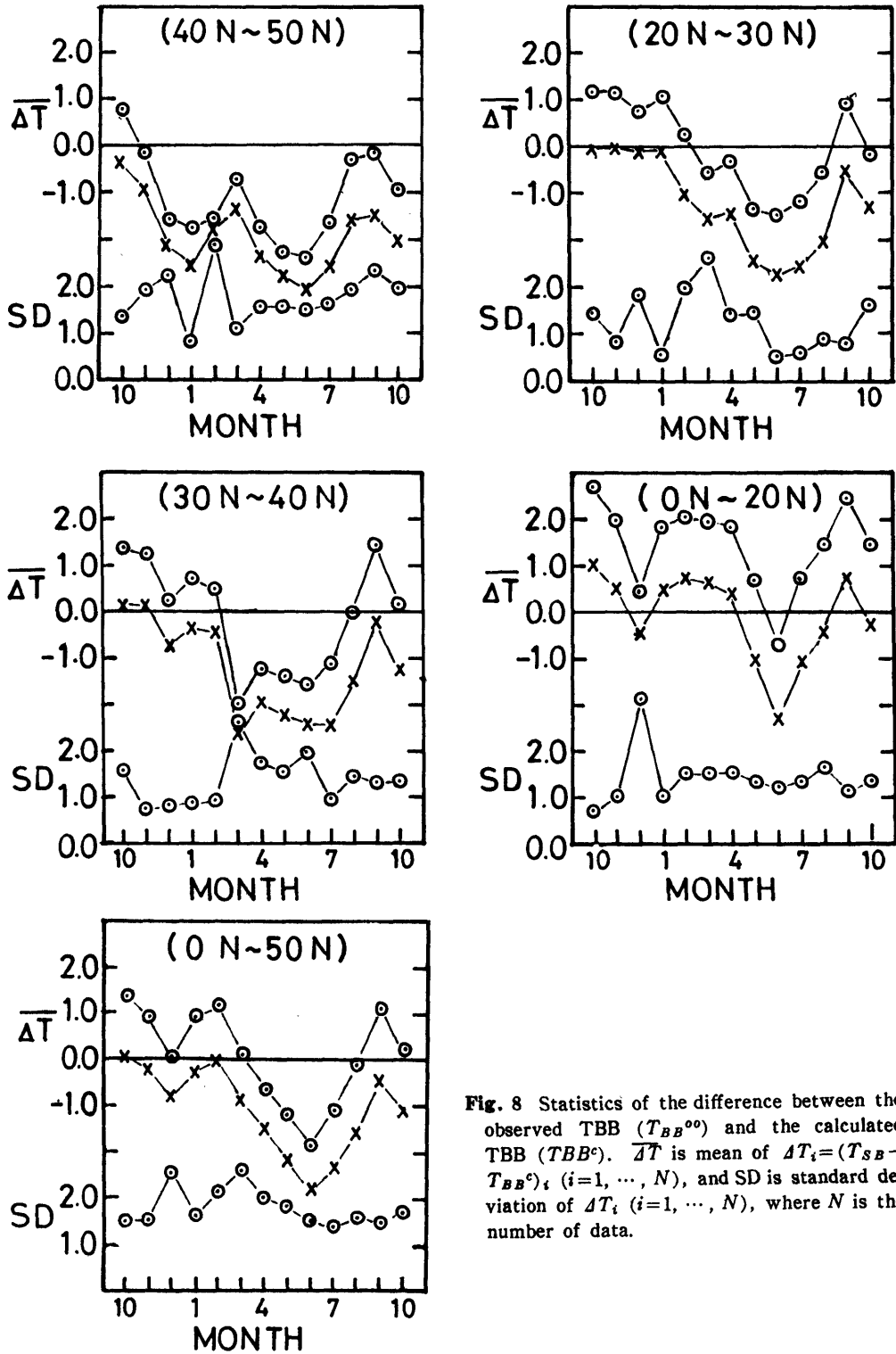


Fig. 8 Statistics of the difference between the observed TBB (T_{BB}^o) and the calculated TBB (T_{BB}^c). $\overline{\Delta T}$ is mean of $\Delta T_i = (T_{SB} - T_{BB}^c)_i$ ($i=1, \dots, N$), and SD is standard deviation of ΔT_i ($i=1, \dots, N$), where N is the number of data.

and the standard deviation of those. \odot and \times indicate the value for $\gamma=0.005$ and $\gamma=0.0$, respectively. Half of mean of the differences are coincident within 1 K, but that sometimes reaches to 2 to 3 K. In the lower latitude zone between 0°N and 20°N , many of data have positive error. A large part of these data are based on the observation at Xishadao (59981). The clear T_{BB} observed near this station has a tendency to high values due to the influence of small islands and coral reefs, or SST of the Ten-Day Marine Report near this station have a tendency to low values because the Ten-Day Marine Report does not include exactly the small structure affected by local geographical features. There is another possibility. We can only observed the radiance which comes from just near surface.

(c) calibration of radiometer on GMS-3

In Fig. 8, it is found that the means of differences in the period from May to June tend to large negative values. The difference greater than 2 K is rather large. This indicates that the errors of the radiative transfer model would be several percents. The differences cannot be solved by adjusting parameters on absorption coefficients in the radiative transfer scheme. Since $\gamma=0.005$ means a large continuum absorption, it is not realistic that radiative transfer scheme has the larger absorption coefficients than this one. Even if aerosol is taken into account, we can improve a difference only to a degree of 1 K.

These facts suggest that the infrared data would not be well-calibrated. It is well-known that infrared data of GMS are not well-calibrated due to the thermal gradient within the sensor unit. Ichiki et. al. (1984)

mentioned the error for the calibration of infrared image data by comparing the simultaneous observation of GMS and GMS-2. Uchiyama et. al. (1984) investigated the relationship among the effective shutter temperature and temperatures in the sensor unit concerning GMS-2 on the base of the radiance calculated theoretically. GMS-3 has the thermal structure similar to GMS-2. The error of effective shutter temperature from May to June are 1.5 to 2.0 K with respect to GMS-2. These differences compensate a large part of errors shown in Fig. 8. The calibration error explains that the systematic error of the first ten days in June is negative almost all over areas.

(d) vertical profile of temperature and water vapor

When we estimate SST from only one infrared channel, the information on the atmosphere must be given from the other source of data; radiosonde data, sounding data derived from orbital satellite, climate value, numerical prediction and so on. As long as we are restricted to the use of the only one infrared channel, the accurate vertical profile cannot be obtained. We need the robust algorithm for error of the vertical profile.

The vertical profile above the ocean is dependent on sounding data derived from polar orbital satellites. If the vertical profile were depend heavily on the orbital satellites, there would be no meaning to retrieve SST from the geostationary meteorological satellites, because we could obtain the more accurate SST from the data observed by the polar orbital satellites; for example, by the method of multi-channel technique using AVHRR data of NOAA/

TIROS series satellites.

Using McClatchy's tropical atmosphere, we tried to estimate the influence of the error of the vertical profile on the observed T_{BB} . The change of temperature by 2 K below the level of 800 mb leads to the change of T_{BB} by about 1 K. The change of water vapor amount by 10% leads to the change of T_{BB} by about 0.4 K. Judging from these results, we cannot avoid the error to a degree of 0.5 to 1 K.

In the new system, the result of objective analysis for numerical prediction is used as the vertical profile of temperature and water vapor instead of climate value. This improves the accuracy of the amount of atmospheric correction. We compared the clear T_{BB} observed by GMS-3 with the cal-

culated T_{BB} using the vertical profile analyzed objectively for numerical prediction, in order to check whether it is proper to use that profile. The means of differences between the observed T_{BB} and the calculated T_{BB} are shown in Fig. 9, 10, 11, and 12 in the period of the first ten days of January, April, June and October in 1985. The differences sometimes exceed 2.0 K, but they are less than 2.0 K almost all over the area. These results do not necessarily show that the vertical profile and the radiative transfer scheme are proper. However, since we are restricted to the use of the only one infrared channel, it is difficult to desire a more accurate value for correcting the atmospheric effect.

We use the vertical profile analyzed ob-

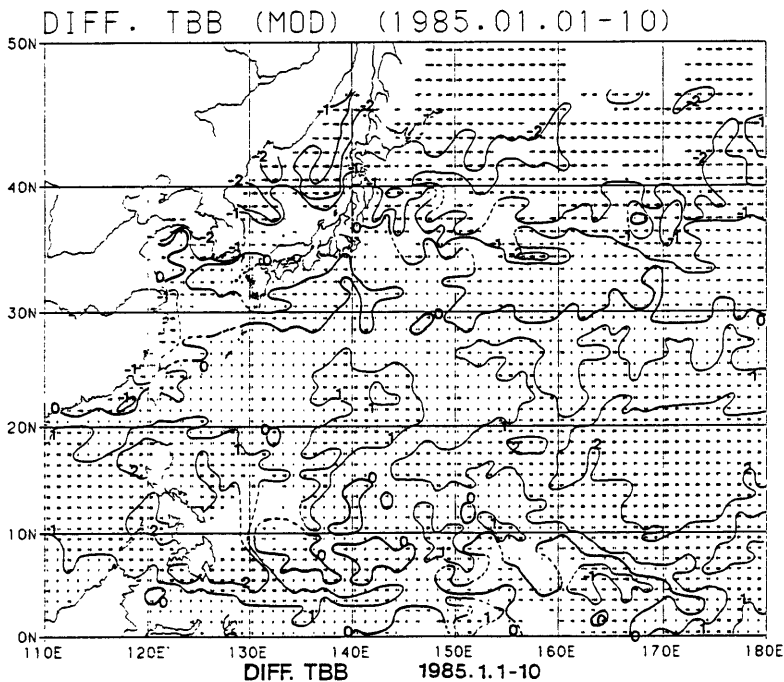


Fig. 9 Mean of difference between the observed TBB using the vertical profile analyzed objectively for numerical prediction, in the period of the first ten days of January in 1985. The value is the former TBB minus the latter one.

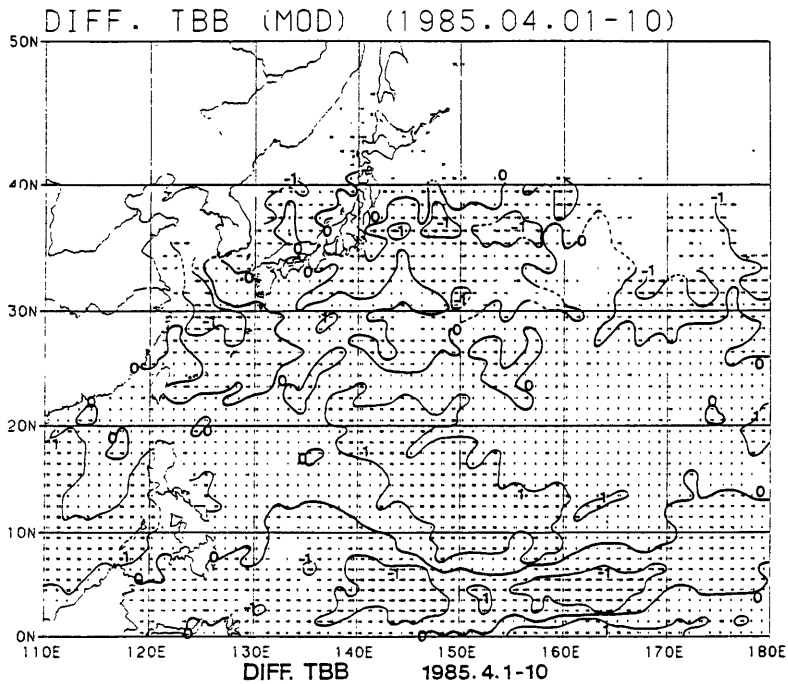


Fig. 10 As in fig. 9, except for April in 1985.

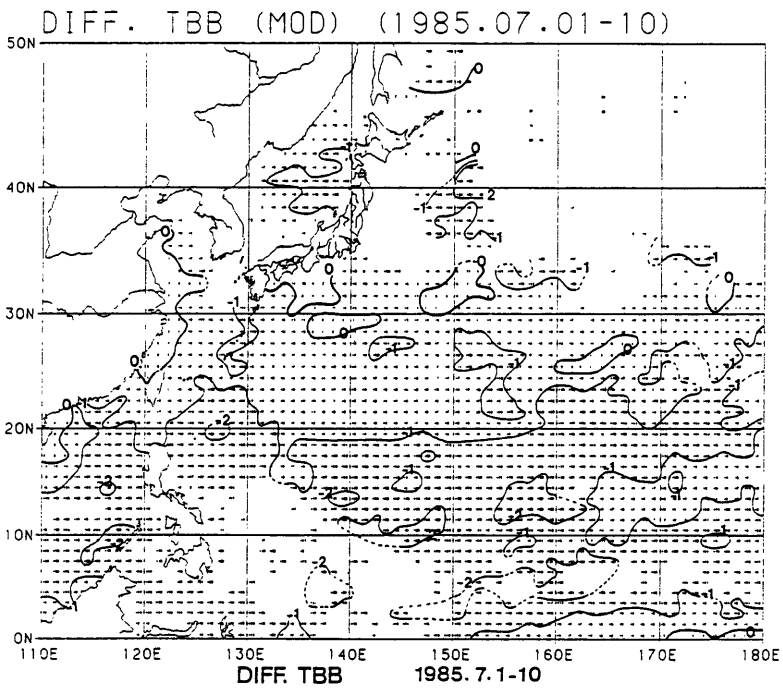


Fig. 11 As in fig. 9, except for July in 1985.

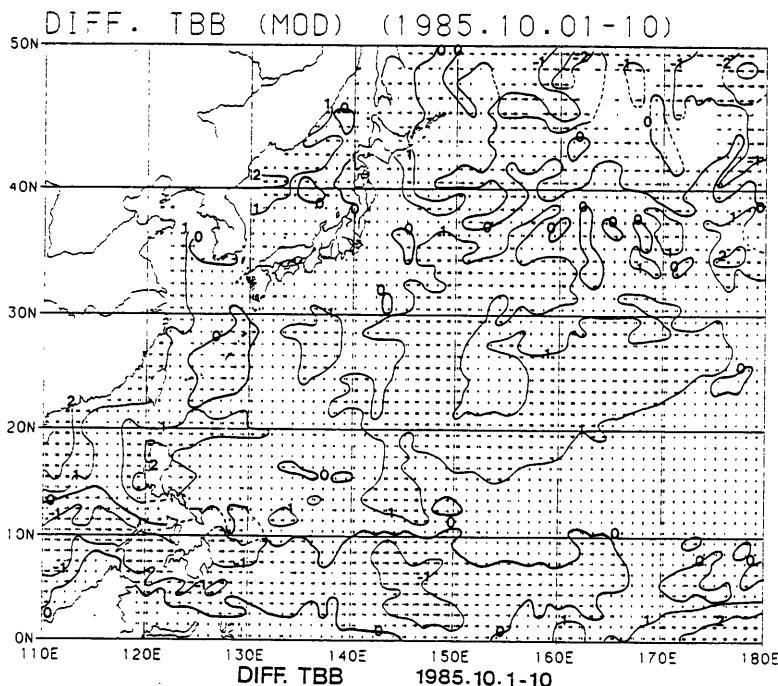


Fig. 12 As in fig. 9, except for October in 1985.

jectively for numerical prediction all over the region. Since water vapor amount is large in the cloudy region, there is a possibility to over-estimate the absorption due to water vapor. The vertical profile in the cloudy region must be modified.

(e) amplification of small error

We cannot specify which factor causes the most serious error. However, the error to a certain degree, ± 1 K, cannot be avoided. The error of the clear T_{BB} , the radiative transfer scheme, and the calibration of radiometer tend to lead the systematic error of SST. Furthermore, since the vertical profile is given every $2.5^\circ \times 2.5^\circ$, its error leads to the error spread widely. The magnitude of error 1 K leads to the serious error of SST because of the reason described below; i. e. a small error is amplified

and the error of SST becomes large.

Fig. 13 and 14 show how the observed T_{BB} changes as the surface temperature changes in McClatchy's tropical atmosphere and mid-latitude summer one, respectively. In these calculation, the vertical profiles of temperature and water vapor are fixed and $\gamma=0.005$ is used. \odot indicates the case where surface temperature is equal to that of the lowest atmospheric level.

As shown in Fig. 13 and 14, the change of radiance observed for the change of surface temperature becomes dull; i. e. dT_{BB}/dT_S is less than 1.0. This indicates that when the earth is observed from the satellite, its contrast become worse than that of the original surface temperature. In the tropical case, the value of dT_{BB}/dT_S is 0.3 to 0.4. For example, $dT_{BB}/dT_S=0.4$ means

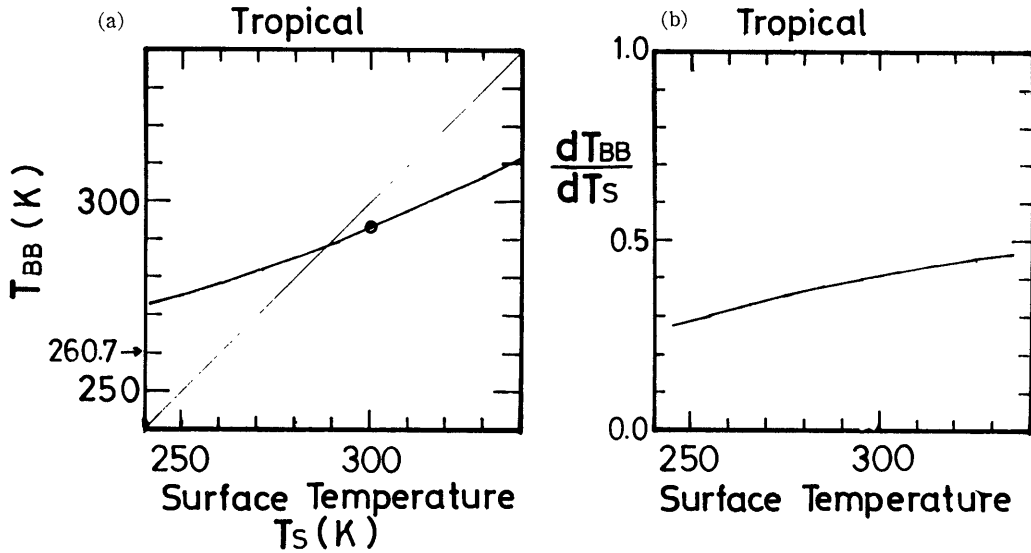


Fig. 13 (a) Relation between surface temperature and the brightness temperature to be observed in the case of McClatchy's tropical atmosphere. The contrast of observed TBB becomes worse than that of the original surface temperature. $T_{BB}=260.7$ is the contribution of atmospheric radiation. (b) Change rate of the observed TBB to the surface temperature. The inverse of this value means an amplification factor of error.

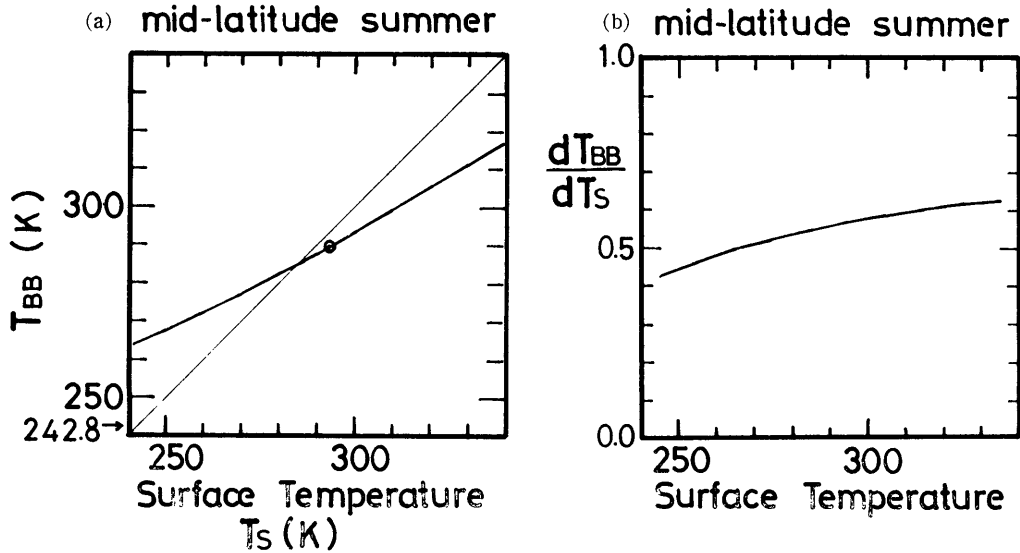


Fig. 14 As in Fig. 13, except for McClatchy's mid-latitude summer atmosphere. $T_{BB}=242.8$ is the contribution of atmospheric radiation.

that when we estimate SST, the error of T_{BB} is amplified by $1/0.4=2.5$ times. In the case that the atmosphere is more wet and the zenith angle of satellite is large, dT_{BB}/dT_S becomes 0.2 to 0.3; i.e. the error of T_{BB} is amplified by 5 to 3 times. The value of dT_{BB}/dT_S in the mid-latitude summer is larger than that of tropical atmosphere, but its value is about 0.5 and the error is amplified by about 2 times. Therefore, even if the error of the clear T_{BB} and the calculated T_{BB} would be ± 1 K, the error of SST becomes ± 2 to 5 K.

The radiometric resolution of infrared sensor on GMS is 0.5 K in the vicinity of 300 K. Therefore, to which count value the observed radiance is converted or digitalized is an important problem. The difference of only one digitalized count leads to the error 1 to 3 K of SST.

The transmittances of the vertical path for McClatchy's tropical atmosphere are shown in Fig. 15. Even in the region of $11 \mu\text{m}$ infrared atmospheric window, transmittances reduce to 0.2 to 0.5 in the case

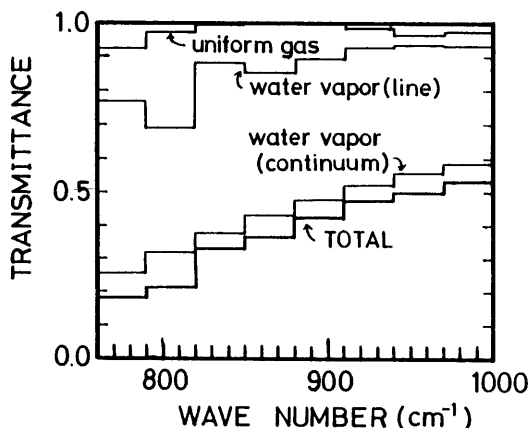


Fig. 15 Transmittances of the vertical path for McClatchy's tropical atmosphere in the region of $11 \mu\text{m}$ region. $\gamma=0.005$ is used (see text.).

that the atmosphere is wet and the path length is long. The ratio of the radiance which is emitted from surface and reaches to the satellite to the observed radiance is about 40% and 60% for McClatchy's tropical atmosphere and mid-latitude summer one, respectively.

The test results show that the new method does not necessarily improve the accuracy of the current operational method. As long as we are restricted to the utilization of the only one infrared channel, many assumptions must be made and the error of the clear T_{BB} and that of the atmospheric correction cannot be avoid to a certain degree. The new method is superior to the current operational method in each procedure. The current operational method implicitly has the empirical tuning proceses and the SST derived by the current method does not go away from the climate value. The inherent amplification nature is hidden from sight with a cover. The new method has not a tuning process. In spite of the more accurate value of clear T_{BB} and the atmospheric correction, the larger error ocured due to the inherent amplification nature. This general concept is shown in Fig. 16. A circle represents a standard of dispersion; i.e. a standard deviation of error and a standard deviation of climate value. The circles of the value obtained by the new method are smaller than those by the current operational one, and a distance between the true value and the estimated one by the new method is nearer than that by the current operational method. However, the distance between the true SST and the estimated SST by the new method is as distant as that by the current one. Further-

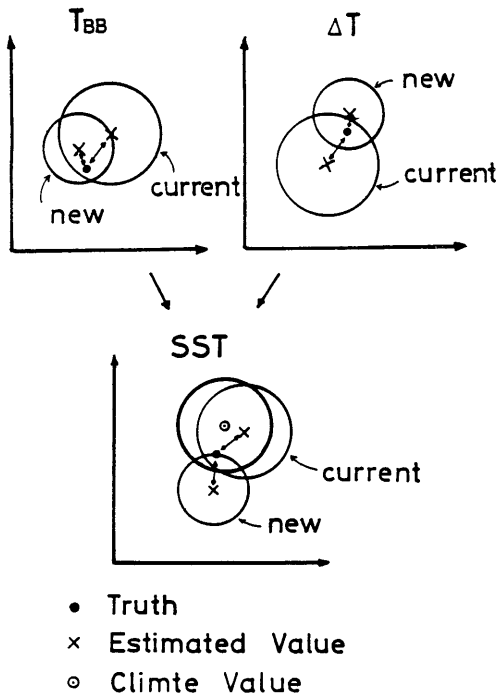


Fig. 16 The schematic view of the general concept on errors. T_{BB} , T and SST are a clear observed TBB, amount of atmospheric correction, and sea surface temperature. ●, ×, and ⊙ mean the truth value, the estimated value, and the climate value, respectively. The size of circle indicates a standard deviation of error and that of climate value.

more, note that the standard deviation of the current method is the same order as the climate value.

5. Conclusion and summary

We developed the new method to correct the atmospheric effect. In the new method, we utilize the vertical temperature and water vapor analyzed objectively for numerical prediction and the solution of radiative transfer equation. We tried to estimate the SST in the four cases in order to investigate the performance of the new method. In every test, the error of SST becomes greater than 2 K over a wide range of area. We

could not estimate exactly the errors in each quantity because of the error of the calibration. The errors of the clear T_{BB} observed by the satellite, and those of the calculated one are probably about 1 K. However, when we convert the clear T_{BB} to SST, the error of the clear T_{BB} and that of the atmospheric correction is amplified by a several times. This feature is inherent.

This fact indicates that the accuracy required for the measurements is less than 0.1 K and multi-channel measurements are necessary to the atmospheric correction in order to remove atmospheric effect by the own measurements only. We cannot use operationally this new method at the present stage. Before this new method is installed, we intend to develop the method to correct the above error using ship and buoy measurements and climate value.

Acknowledgements

We wish to thank Mr. T. Yoshida, Head of Sapporo District Meteorological Observatory, for encouraging us always in our study when he was Director of Japan Meteorological Satellite Center last year. We also very grateful to Mr. I. Kubota for the continuing support when he was Head of our department last year. Also, numerous discussions with Dr. A. Mita and Mr. Y. Takeuchi are greatly appreciated.

References

Ichiki, A., M. Togashi and A. Uchiyama, 1984: An Analysis of the Data Obtained by a Simultaneous Observation of GMS and GMS-2. —A Study of the Difference between the Brightness Temperatures by GMS and Those by GMS-2—, Meteorological Satellite Center Technical Note No. 10, 19-27 (in Japanese).
 Inoue, T., 1979: Empirical Atmospheric Correc-

- tion, Meteorological Satellite Center Technical Note (Special Issue II-2), Summary of GMS System, II Data Processing, Part 2, 7-14 (in Japanese).
- Kneizys, F. X., E. P. Shettle, W. O. Gallery, J. H. Chetwynd Jr., L. W. Abreu, J. E. A. Selby, R. W. Fenn and R. A. McClatchey, 1980: Atmospheric Transmittance/Radiance: Computer Code LOWTRAN 5, AFGL-TR-80-0067, Air Force Geophysics Laboratory, Hanscom AFB, MA, 233pp.
- McClatchey, R. A., R. W. Fenn, J. E. A. Selby, F. E. Volz, and J. S. Garing, 1972: Optical properties of the atmosphere (third edition), AFCRL-72-0497, Air Force Cambridge Research Laboratories, L. G. Hanscom Field, Bedford, MA, 108 pp.
- Roberts, R. E., J. E. A. Selby and L. M. Biberman, 1976: Infrared continuum absorption by atmospheric water vapor in the 8-12 μm window, Appl. Opt., 15, 2085-2090.
- Selby, J. E. A., F. X. Kneizys, J. H. Chetwynd Jr., and R. A. McClatchey, 1978: Atmospheric Transmittance/Radiance: Computer Code LOW-TRAN 4, AFGL-TR-78-0053, Air Force Geophysics Laboratory, Hanscom AFB, Bedford, MA, 100 pp.
- Smith, W. L., 1969: A polynomial representation of carbon dioxide and water vapor transmission. ESSA Technical Report NESC 47, Environmental Science Services Administration, U.S. Department of Commerce, Washington, D. C., 20 pp.
- Uchiyama, A., A. Ichiki and T. Takahashi, 1984: VISSR Infrared Calibration by Means of Calculated Radiances, Meteorological Satellite Center Technical Note No. 10, 29-36 (in Japanese).
- Weinreb, M. P. and M. L. Hill, 1980: Calculation of Atmospheric Radiances and Brightness Temperatures in Infrared Window Channels of Satellite Radiometers, NOAA Technical Report NESS 80, National Oceanic and Atmospheric Administration, U. S. Department of Commerce, Washington, D. C., 40 pp.
- Weinreb, M. P. and A. C. Neuendorffer, 1973: Method to apply homogeneous-path transmittance models to inhomogeneous atmosphere, J. Atmos. Sci., 30, 662-666.

GMS の赤外画像データによる海面水温の推定

内山 明博*・藤村 弘志**
用 貝 敏 郎***

GMSの赤外画像データから、海面水温を推定する際の大気補正の方法と、それを使って得られた結果について述べる。

現在、GMSの赤外画像データの大気補正は、経験式と気候値の可降水量を使って計算している。新しい方法では、大気鉛直温度・水蒸気分布として数値予報の解析値を使い、大気補正值は放射伝達方程式を解くことによって計算する。

新しい方式で海面水温の推定を4例行った。その結果、系統的誤差(広い領域にわたって同じ傾向の誤差)が生じやすいことがわかった。誤差の大きさは、5Kを超えることもあり、定量的な解析に耐え得るものでない。これは、観測 T_{BB} や計算 T_{BB} の誤差が、海面水温を推定するとき増幅されるためである。この性質は、衛星から海面水温を推定する際の本質的な性質であり、1チャンネルの画像データからの海面水温の推定は非常に困難であることを示している。

これらのことから、海面水温を精度0.5K以下で推定するには、晴天 T_{BB} (雲の影響を受けていない衛星到達放射)、大気補正值を精度0.1K以下で決める必要がある。さらに大気鉛直分布について仮定することなく、衛星の測定だけから大気補正を行うことが望ましく、いくつかの波長域で地球からの放射を測定する必要がある。

- * 気象衛星センター・システム管理課
- ** 気象衛星センター管制課(現所属、科学技術庁)
- *** 気象衛星センター解析課